We are IntechOpen,
the world's leading publisher of
Open Access books
Built by scientists, for scientists

6,900
Open access books available

186,000
International authors and editors

200M
Downloads

154
Countries delivered to

Our authors are among the

TOP 1%
most cited scientists

12.2%
Contributors from top 500 universities

CLARIVATE ANALYTICS
BOOK CITATION INDEX
INDEXED

WEB OF SCIENCE™

Selection of our books indexed in the Book Citation Index
in Web of Science™ Core Collection (BKCI)

Interested in publishing with us?
Contact book.department@intechopen.com

Numbers displayed above are based on latest data collected.
For more information visit www.intechopen.com

TiO$_2$ Nanoparticles Prepared by Sol-Gel Method for Anode Application in Lithium-Ion Batteries

Wafaa Nachit, S. Touhtouh, Z. Ramzi, K. Benkhouja and R. Yazami

Abstract

TiO$_2$ nanoparticles are prepared via sol-gel method using titanium tetraisopropoxide (TTIP) as a precursor under refluxing and controlled pH. It is found that pure anatase phase is obtained with pH 10. Further characterization studies are carried out on pure nanoparticle anatase phase by XRD, SEM, and transmission electron microscope (TEM). Their electrochemical performances as anode material in lithium-ion batteries are investigated by cyclic voltammetry, galvanostatic cycling, and rate capability measurements. A high discharge capacity of 321 mAh/g (vs. 335 mAh/g theoretical) is achieved at 1C rate. After the first galvanostatic charge/discharge cycle, voltage profiles show plateaus at 1.75 and 1.95 V versus Li at discharge and charge, respectively. High Coulombic efficiency (>99%) is maintained after 300 cycles, which makes anatase TiO$_2$ nanoparticles prepared by sol-gel method, a very promising material for anode application in lithium rechargeable batteries.

Keywords: TiO$_2$ nanoparticles, anode, lithium-ion batteries, electrochemical characteristics

1. Introduction

Nanostructured titania (NST) TiO$_2$ is a very promising alternative anode material compared with the commercialized lithium titanate L i$_4$Ti$_{15}$O$_{12}$ and graphite materials for lithium-ion battery application in particular when fast charging is required [1–3]. Fast charging while keeping long battery operational life is one of the most challenging tasks in lithium-ion batteries nowadays. Both mobile electronics and electro-mobility sectors need fast charging to compensate for relatively low energy density which impacts the operation time and driving range. One serious option to cope with charging time limitations resides in developing new materials able to store large amounts of lithium in a very short time. Nanomaterials, including NST, are among the most promising in this regard.

Good performances of NST result from their outstanding characteristics such as:

i. A low volumetric change upon lithium-ion intercalation and de-intercalation providing a high crystal structure stability and long cycle life

ii. A fast diffusivity of lithium ions within the TiO_2 structure providing fast charging and high power discharge

iii. A practical low operating voltage

iv. An enhanced safety

Several methods have been used for the synthesis of NST, including hydrothermal [4–10], sol-gel [5–11], hydrolysis [12, 13], atomic layer deposition [14], and anode deposition [15], for the most reported in the literature. According to the synthesis method and to the post-thermal treatment conditions, NST of different morphologies are obtained such as nanorods [4, 17], nanotubes [5–6, 8–9, 14, 17], nanofibers/nanowires [11–20], nanoparticles [6, 7, 10], nanocomposites [12, 21], nanofilms, and nanosheets [15, 22].

Several polymorphs of TiO_2 are known such as tetragonal rutile and anatase, orthorhombic brookite, and monoclinic $TiO_2(B)$ [23]. Anatase and $TiO_2(B)$ have open-channel structure and show high cycle capacity compared to rutile TiO_2 [24]. Anatase has edge-sharing TiO_6 octahedra so that planar double chains are formed with a tetragonal body-centered space group ($I4_1/amd$) [25].

Li-ion diffusion in anatase occurs along the octahedral interstitial sites up to $Li_{0.5}TiO_2$ composition. Then the tetragonal structure reversibly transforms to the orthorhombic phase [26–30]. Anatase TiO_2 anode material reversibly uptakes 0.5 Li per TiO_2 formula with lithium insertion/extraction taking place at relatively low voltage and showing fast kinetics [29, 30]. However, 0.5 Li per TiO_2 corresponds to half of theoretical capacity of 335 mAh/g [31–33]. Enhancing practical capacity in NST should make this material more attractive for anode application in lithium-ion batteries [34].

When wet chemistry route is used to prepare NST, the medium pH is of a significant importance in the crystal structure and morphology of the final product [32]. Syntheses of TiO_2 anatase were mostly performed in acidic media usually at pH greater than 4.5 [33]. To the authors' knowledge, there has been no report on sol-gel preparation of NST in alkaline pH.

In this chapter, we show that unlike in acidic pH, which lead to mixed phases, pure anatase NST is obtained via sol-gel at pH 10. NST prepared at different pH are analyzed by XRD, transmission electron microscope (TEM), and SEM. The electrochemical properties of pure anatase phase NST are investigated by cyclic voltammetry and galvanostatic cycling, including rate capability tests in view of its application as anode material in lithium-ion batteries.

2. Experimental

2.1 Sample preparation

NST are prepared via sol-gel method using titanium tetraisopropoxide (TTIP), distilled water, and 2-propanol. Hydrochloric acid and sodium hydroxide are mixed in 24 mL of 2-propanol to fix the pH to 1, 4, 10, and 13 and to control the hydrolysis process of the solution. 24 mL of TTIP is then slowly added to the mixture, followed by refluxing at 70°C to obtain the sol. 10 mL of distilled water is added to the solution and left for 1 h under stir heating.

The obtained gel is dried at 70°C in air and then calcined at 500°C in air to produce NST powders.

2.2 Characterization

NST are characterized by X-ray diffractometry (XRD) using a PR-XPERT diffractometer (PW3064) with CuK$_\alpha$ radiation (λ = 1.5406 Å), operating at 45 kV and 40 mA in 2θ angular range of 10–70°. The morphology and particle size were examined by transmission electron microscope (TEM, JEOL, JEM-2010) and by field-emission scanning electron microscopy (FESEM, JEOL JSM-7600F, 5 kV).

2.3 Electrochemical measurements

The anode is prepared by mixing NST prepared at pH 10 as active material, acetylene carbon black as electronic conductor, and polyvinylidene fluoride (PVDF) as a binder in the weight ratio of 80:10:10 with N-methyl-2-pyrrolidone (NMP) to form a slurry. The slurry was coated on a copper foil by doctor blade and then vacuum dried at 110°C for 6 h. The anode loading is ~0.8 mg cm^{-2}. Lithium half-cells are assembled in a glove box under ultra-dry argon atmosphere (<1 ppm H$_2$O and O$_2$). Lithium metal was used as the counter and reference electrode. The electrolyte consisted of 1.0 M LiPF$_6$ solution in ethylene carbonate (EC) and diethyl carbonate (DEC) at a volumetric ratio of 1:1. The separator is microporous polyethylene. Li/NST half-cells are investigated by cyclic voltammetry at 0.2 mV/s sweeping rate and by galvanostatic cycling at 1C–20 C rates, all between 1.0 V and 3.0 V versus Li.

3. Results and discussion

3.1 Physical characterizations

Figure 1 shows the XRD patterns of TiO$_2$ nanoparticles prepared at pH 1, 4, 10, and 13 and calcined at 500°C. X-ray patterns of anatase, rutile, and brookite are shown for reference.

The sample prepared at pH 1 consists mostly of the rutile phase. All other samples are anatase with brookite impurities at pH 4 and 13. TiO$_2$ nanoparticles synthesized at pH 10 consist of highly crystalline anatase phase (00-004-0477). **Table 1** summarizes the XRD data of TiO$_2$ nanoparticles synthesized at pH 10 including diffraction peak 2θ, interlayer spacing "d," and hkl indexes. **Table 2** gives the crystallographic characteristics of TiO$_2$ anatase phase prepared at pH 10 as derived from the XRD data Rietveld refinement. Average crystallite sizes of nanoparticles synthesized at different pH are reported in **Table 3** using Scherrer's equation. The particle size is in ~20–30 nm range with no obvious trends versus pH.

Figure 2 shows TEM images of TiO$_2$ nanoparticles prepared at pH 10 at different magnifications. **Figure 2a** and **b** shows primary particles with relatively narrow size distribution. High-resolution TEM of **Figure 2c** shows the polycrystalline nature of the TiO$_2$ nanoparticles with well-resolved layers such as those assigned to the orientation corresponding to an interlayer of about 0.36 nm as indicated by an arrow.

TEM image analysis allows particle-size distribution to be determined as shown in **Figure 3**. The particle-size distribution is built on a discrete set of clearly identifiable grains, and, therefore, it is not necessarily representative of the overall description of the sample. This is especially true for grain sizes close to the distribution tails where the probability of finding a very large or a very small grain under the TEM objective is rather low. The average size of about 17 nm is slightly lower than the one estimated from the XRD data.
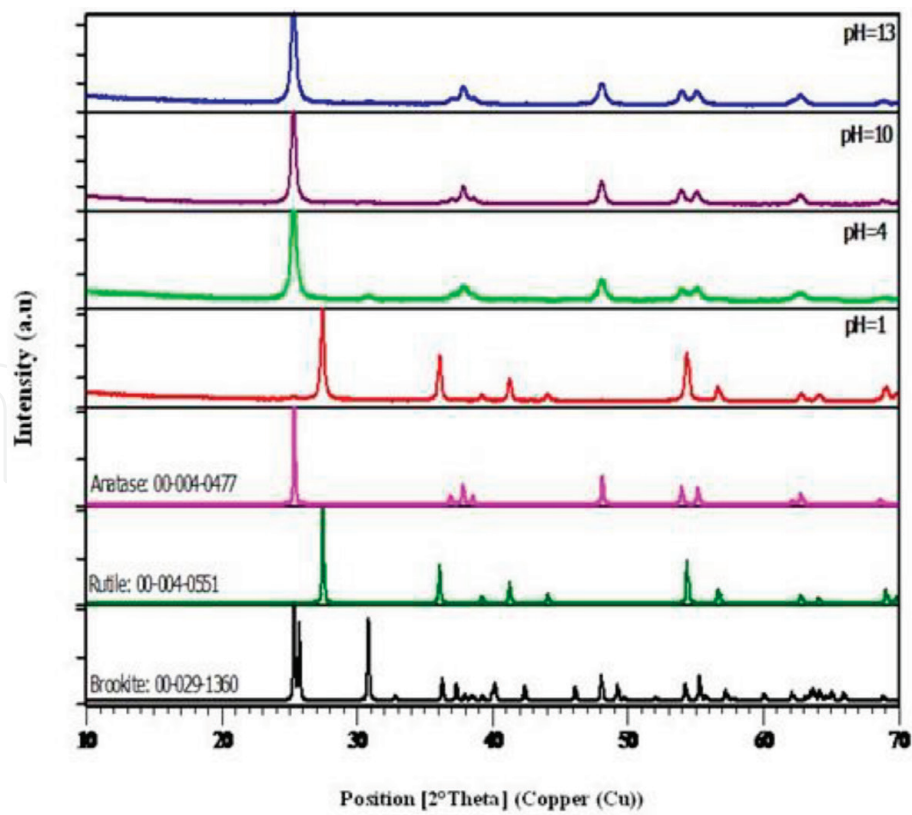
Figure 1.
XRD patterns of titania nanoparticles made at different pH. Anatase, rutile, and brookite spectra are also shown for reference.

2θ (°)	d (nm)	(hkl)
25.31	0.3518	(101)
36.98	0.2430	(103)
37.82	0.2378	(004)
38.61	0.2331	(112)
48.05	0.1893	(200)
53.92	0.1700	(105)
55.09	0.1637	(221)
62.13	0.1494	(213)
62.70	0.1481	(204)
62.80	0.1479	(116)

Table 1.
Indexation of XRD peaks on TiO$_2$ nanoparticles obtained at pH 10.

SEM images of NST pH 10 are displayed in **Figure 4a** and **b**. High magnification **Figure 4a** shows primary particles with narrow size distribution aggregate into secondary particles of about 150–600 nm in size, whereas lower magnification **Figure 4b** shows agglomerated particles remain basically submicron in size.

3.2 Electrochemical characterizations

Figure 1a shows cyclic voltammograms of the Li/NST of pH 10 half-cell at 0.2 mV/s sweeping rate for 5 cycles. In the first cycle, two reduction peaks appear at 2.15 V and at 1.75 V, respectively, whereas only one re-oxidation peak is present at 2.10 V.

Phase	α β γ	Lattice parameters	
Anatase (Tetragonal I41)	α = β = γ = 90°	a = b = 3.783	c = 9.5190

Table 2.
Characteristics of anatase crystal structure.

pH	Phase	D (nm)
1	Anatase-rutile	32.0
4	Anatase-brookite	21.3
10	Anatase	26.2
13	Anatase-brookite	21.3

Table 3.
Crystallite size of TiO₂ nanoparticles synthesized at different pH.
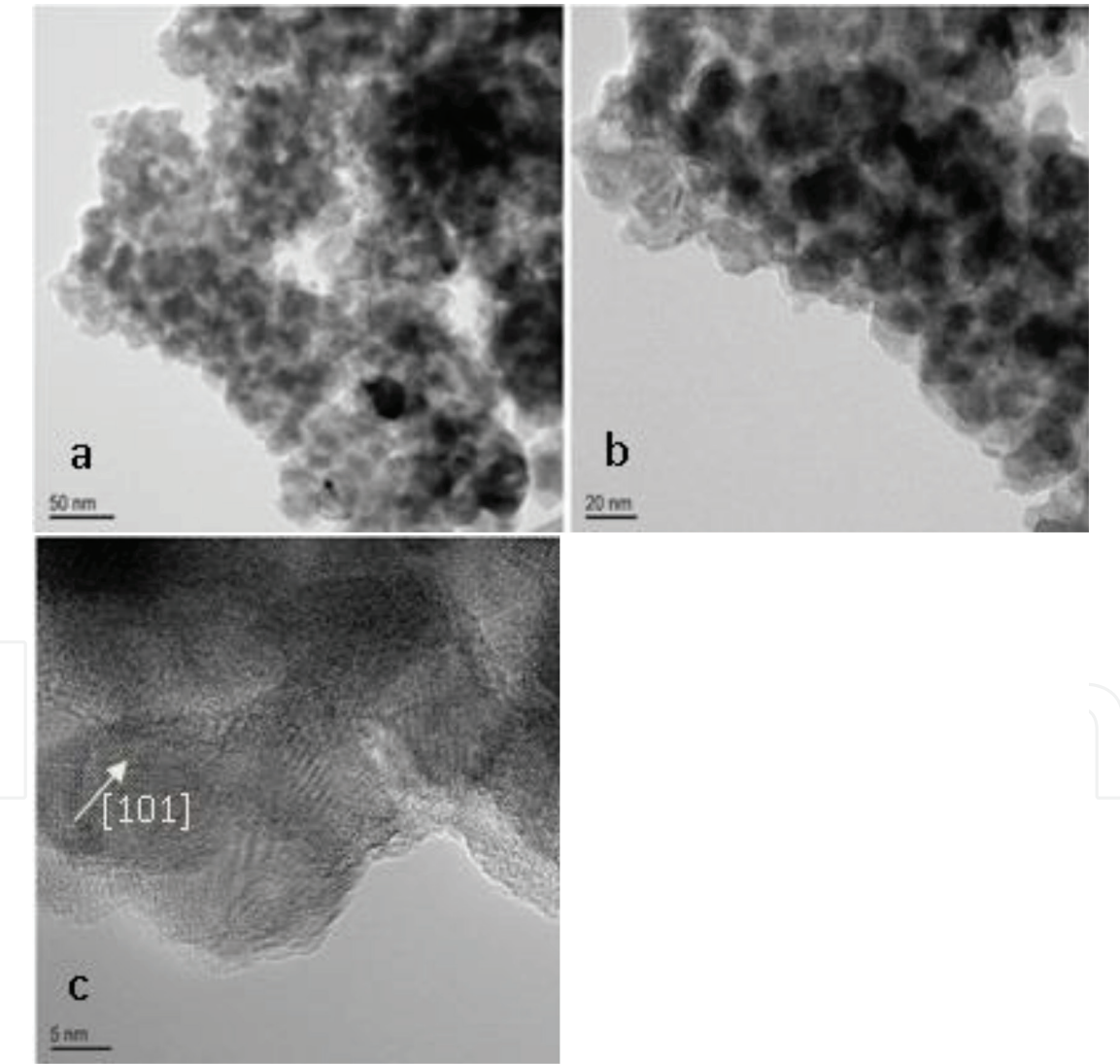
Figure 2.
TEM images at different magnifications of TiO₂ nanoparticles prepared at pH 10. (a, b) Image analysis enables size distribution to be achieved. HR-TEM image of (c) shows polycrystalline structure with some preferred layer orientation such as with interlayer spacing of about 3.6 nm.

In the following 4 cycles, only the reduction peak at 1.75 V and re-oxidation peak at 2.10 V appeared. The first reduction peak at 2.15 V accounts for about 50% of the total discharge capacity of about 320 mAh/g, which is close to theoretical capacity
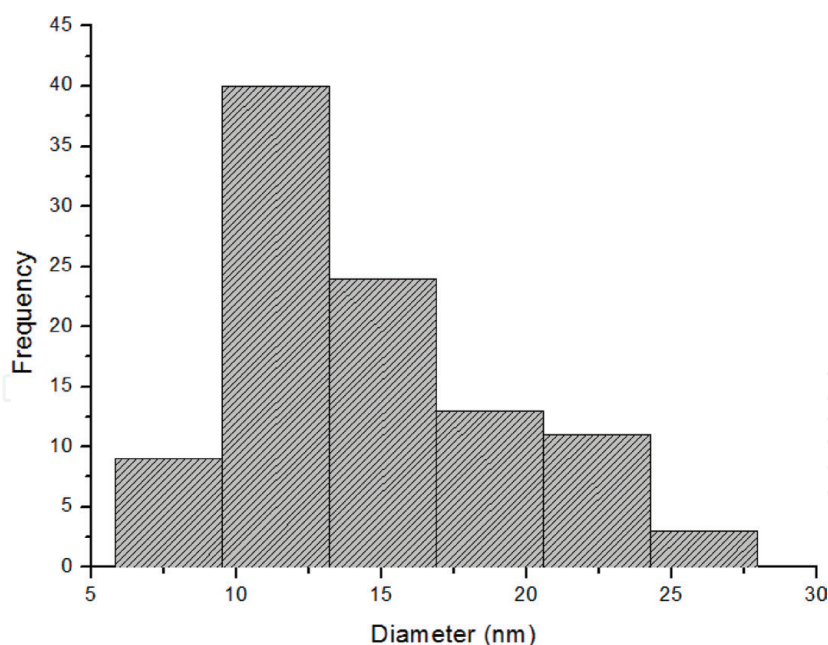
Figure 3.
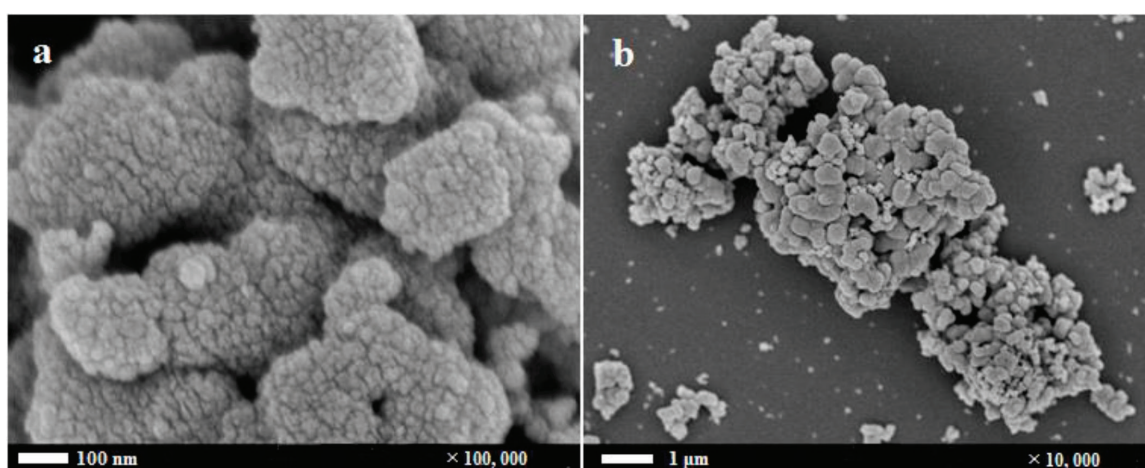*Grain size distribution for the TiO₂ at pH 10 from the TEM image analysis.*

Figure 4.
SEM images of TiO₂ nanoparticles synthesized at pH 10.

of 335 mAh/g of TiO_2 corresponding to 1 Li/TiO_2 ratio. The second reduction peak at 1.75 V accounts for the second half of the total capacity and is matched by the re-oxidation peak at 2.1 V. This situation remained almost unchanged during the four following cycles, that is, the capacity of the reduction peak at 1.75 V matches the one of the re-oxidation peaks at 2.1 V of about 140 mAh/g.

The data shown above are confirmed during the two first galvanostatic cycles of the Li/NST cell displayed in **Figure 5b**. The first discharge profile shows two semi-plateaus at about 2.15 and 1.75 V, respectively, whereas the charge profile shows a main plateau at about 2.0 V. The first discharge semi-plateau accounts for nearly half of the total discharge capacity. The second half discharge capacity is matched by the charge capacity.

Cyclic voltammetry and galvanostatic data suggest a two-step electrode reaction process:

1. Irreversible formation of $Li_{0.5}TiO_2$ at ~ 2.15 V average voltage.

2. Reversible formation of Li_1TiO_2 from $Li_{0.5}TiO_2$ at ~ 1.75 V. During re-oxidation $Li_{0.5}TiO_2$ is formed from Li_1TiO_2 at about 2.1 V.
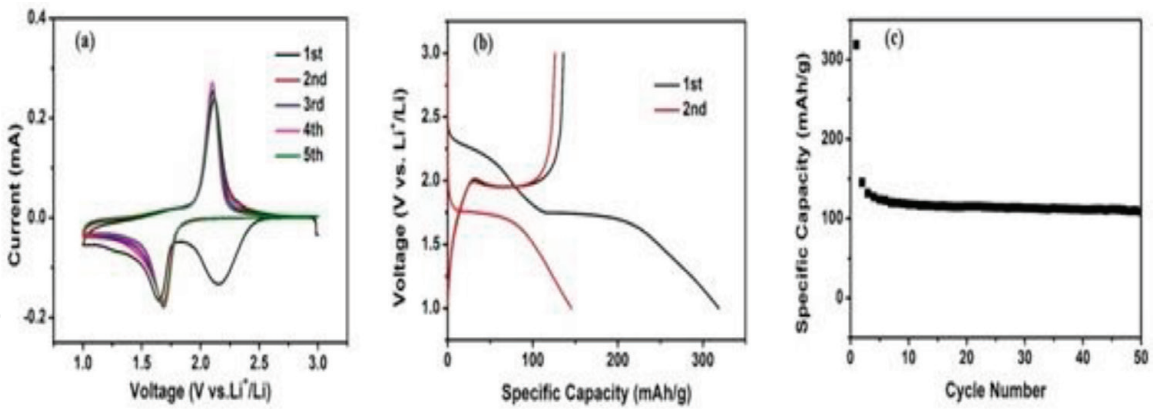
Figure 5.
Electrochemical tests performed on Li/TiO₂ (pH 10) half-cells. (a) Cyclic voltammograms (CVs) at a scan rate of 0.2 mV/s for the first 5 cycles within a potential range from 1 to 3.0 V (vs. Li/Li⁺), (b) discharge-charge capacity of the first and second cycles at a specific current of 175 mA/g (1C), and (c) cycle capacity profile at 1C rate for 50 cycles.
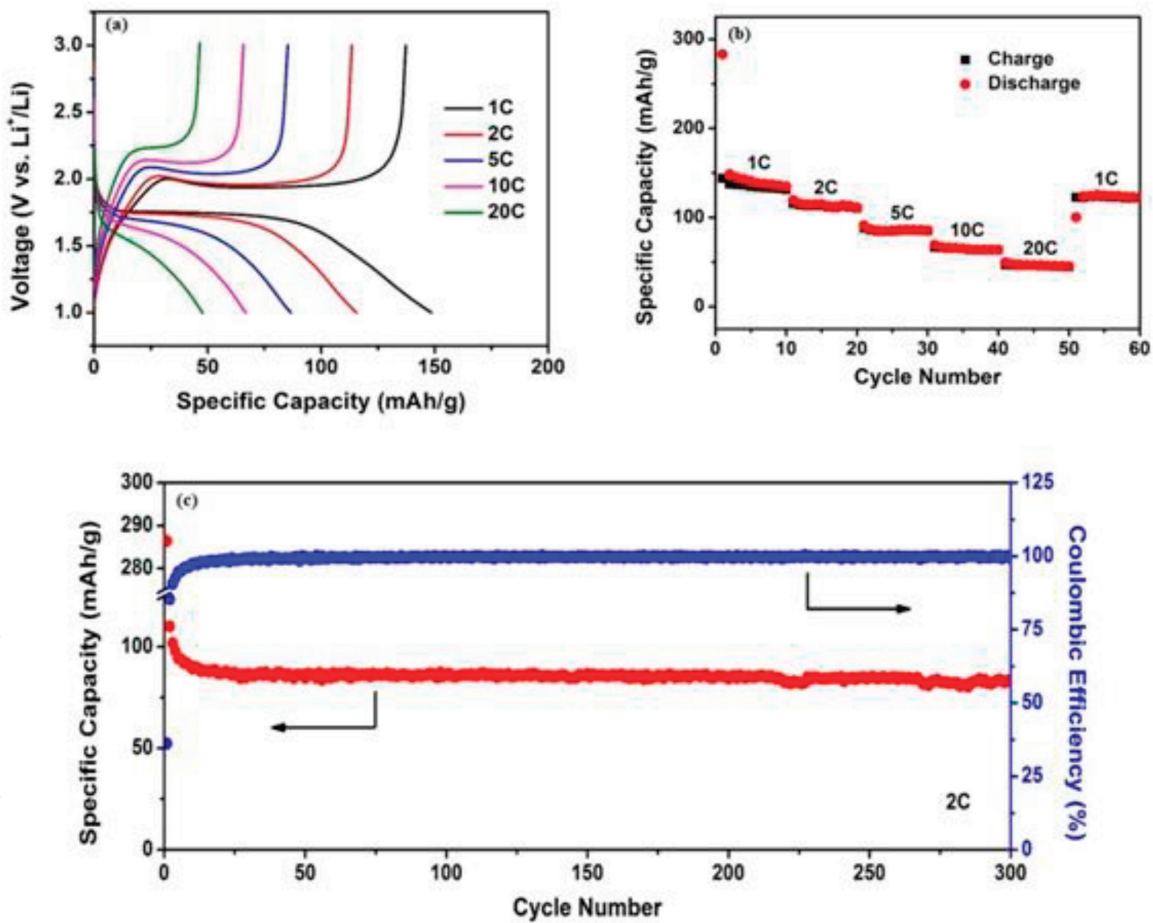

Figure 6.
Rate capability (1C–20C) tests performed on Li/TiO₂ (pH 10) half-cells. (a) Discharge-charge voltage profiles, (b) discharge-charge capacity profile, and (c) cycle capacity and Coulombic efficiency profiles at 2C rate.

The formation of lithium-rich Li_1TiO_2 is supported by both theoretical and experimental data [30–35]. In the anatase phase, orthorhombic $Li_{0.5}TiO_2$ and distorted rock-salt structure Li_1TiO_2 in which lithium cation occupy the octahedral sites have been stabilized due to kinetic effects. Metastability has been reported in Li-poor TiO_2 [30]. Accordingly, our data are consistent with reversible lithium intercalation in the stoichiometry range $0.5 < x < 1$ in anatase Li_xTiO_2, which corresponds to a theoretical capacity of 167.5 mAh/g. The cycle capacity profile in

Figure 5c shows a plateau at about 120 mAh/g at 350 mA/g rate. A lower capacity may be due to limitation in lithium uptake to $Li_{0.85}TiO_2$ and $Li_{0.7}TiO_2$ as reported in [36, 37].

The intercalation mechanism of Li ions into anatase has been studied in a variety of experimental and theoretical works [38]. The lithium-ion intercalation can be described by the following Eq. (1):

$$TiO_2 + xLi^+ + xe^- \rightarrow Li_xTiO_2 \tag{1}$$
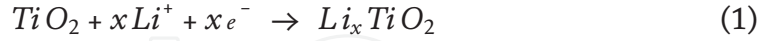
TiO_2 maximum theoretical capacity is 335 mAh/g [39] which corresponds to $x = 1$ and to the complete reduction of Ti^{4+} to Ti^{3+}. This makes TiO_2 a highly competitive alternative to graphite anodes [40].

Practical capacity of anatase TiO_2 is about 200 mAh/g associated with 0.6 Li mole reversible intercalation at 1.78 V versus Li^+/Li [41]. It has been demonstrated that Li_1TiO_2 composition can be obtained from anatase TiO_2 at high temperature [30] or with particle size below 7 nm [42].

The discharge-charge profiles at current rates ranging from 1.0C to 20C and corresponding rate capability profiles are depicted in **Figure 6a** and **b**, respectively. It is worth noticing that after 10 cycles at 20C rate where capacity decreased to about 50 mAh/g, the capacity at 1C rate was recovered during the following 10 cycles to about 137 mAh/g. This indicates a high stability of the anatase TiO_2 nanoparticles based anode toward high rate cycling.

Figure 6c shows the cycle capacity profile at 2C rate for 300 cycles together with Coulombic efficiency. The latter stabilizes close to unity after the first 5 cycles, whereas the capacity gradually dropped to 82.4 mAh/g after 300 cycles indicating the high capacity retention and good cycling stability.

4. Conclusion

TiO_2 nanoparticles are synthesized by simple sol-gel method at different pH values and found to have particle size of 10–30 nm. XRD measurements show that the sample prepared at pH 10 crystallized to pure anatase phase. The TEM and the SEM images confirm the formation of nanoparticles with diameters of 10–30 nm. The TiO_2 nanoparticles prepared at pH 10 exhibit initial capacity of 321 mAh/g and a remarkable high Coulombic efficiency close to unity after 300 cycles at 2C rate. However, the first cycle efficiency is relatively low perhaps due to inherent metastability of Li-poor phases at the early stage of lithium intercalation. More work has currently been performed to improve the first cycle efficiency, therefore making anatase nanoparticles based anode more practical in rechargeable lithium batteries with fast charge and high lithium storage capacity. Among possible routes considered to improve the NTO initial cycle efficiency is the incorporation of a few amounts of lithium during sol-gel process so as to achieve a pre-lithiated phase making it easier to add more lithium during the first cathodic process.

Author details

Wafaa Nachit[1,2], S. Touhtouh[2], Z. Ramzi[1,2], K. Benkhouja[1] and R. Yazami[3*]

1 Laboratory of Coordination and Analytical Chemistry (LCCA (E2M)), Faculty of Sciences, Department of Chemistry, Chouaib Doukkali University, El Jadida, Morocco

2 Engineering Sciences Laboratory for Energy (LabSIPE), National School of Applied Sciences (ENSA), Chouaib Doukkali University, El Jadida, Morocco

3 Energy Research Institute, Nanyang Technological University, Singapore, Singapore

*Address all correspondence to: rachid@ntu.edu.sg and nachit.wafaa@gmail.com

IntechOpen

References

[1] Wang C, Wu LX, Wang H, Zuo WH, Li YY, Liu JP. Fabrication and shell optimization of synergistic TiO_2-MoO_3 core-shell nanowire array anode for high energy and power density lithium-ion batteries. Advanced Functional Materials. 2015;**15**(23):3524-3533

[2] Wei W, Oltean G, Tai CW, Edstrom K, Bjorefors F, Nyholm L. High energy and power density TiO_2 nanotube electrodes for 3D Li-ion microbatteries. Journal of Materials Chemistry. 2013;**1**(28):8160-8169

[3] Ortiz GF, Hanzu I, Lavela P, Knauth P, Tirado JL, Djenizian T. Nanoarchitectured TiO_2/SnO: A future negative electrode for high power density Li-Ion microbatteries. Chemistry of Materials. 2010;**22**(5):1926-1932

[4] Liu YB, Ding TL, Shen DL, Dou J, Wei MD. Hierarchically structural TiO_2 nanorods composed of rutile core and anatase shell as a durable anode material for lithium-ion intercalation. Journal of Electroanalytical Chemistry. 2017;**804**:87-91

[5] Fang J, Liu WW, Yu F, Qin FR, Wang MR, Zhang K, et al. Fe, S co-doped anatase TiO_2 nanotubes as anodes with improved electrochemical performance for lithium ion batteries. RSC Advances. 2016;**6**(74):70133-70,140

[6] Tang YK, Liu L, Zhao HY, Jia DZ, Xie XL, Zhang Y, et al. Anatase/rutile titania anchored carbon nanotube porous nanocomposites as superior anodes for lithium ion batteries. CrystEngComm. 2016;**18**(24):4489-4494

[7] Sanad MMS, Rashad MM, Powers K. Enhancement of the electrochemical performance of hydrothermally prepared anatase nanoparticles for optimal use as high capacity anode

materials in lithium ion batteries (LIBs). Applied Physics A: Materials Science and Processing. 2015;**118**(2):665-674

[8] Choi MG, Lee YG, Song SW, Kim KM. Anode properties of titanium oxide nanotube and graphite composites for lithium-ion batteries. Electrochimica Acta. 2010;**55**(20):5975-5983

[9] Xu JW, Jia CH, Cao B, Zhang WF. Electrochemical properties of anatase TiO_2 nanotubes as an anode material for lithium-ion batteries. Electrochimica Acta. 2007;**52**(28):8044-8047

[10] Oh SW, Park SH, Sun YK. Hydrothermal synthesis of nano-sized anatase TiO_2 powders for lithium secondary anode materials. Journal of Power Sources. 2006;**161**(2):1314-1318

[11] Lee S, Eom W, Park H, Han TH. High-temperature stable anatase titanium oxide nanofibers for lithium-ion battery anodes. ACS Applied Materials and Interfaces. 2017;**9**(30):25332-25,338

[12] Liu JL, Feng HB, Jiang JB, Qian D, Li JH, Peng SJ, et al. Anatase-TiO_2/CNTs nanocomposite as a superior high-rate anode material for lithium-ion batteries. Journal of Alloys and Compounds. 2014;**603**:144-148

[13] Xu W, Wang ZY, Guo ZD, Liu Y, Zhou NZ, Niu B, et al. Nanoporous anatase TiO_2/single-wall carbon nanohorns composite as superior anode for lithium ion batteries. Journal of Power Sources. 2013;**232**:193-198

[14] Panda SK, Yoon Y, Jung HS, Yoon WS, Shin H. Nanoscale size effect of titania (anatase) nanotubes with uniform wall thickness as high performance anode for lithium-ion secondary battery. Journal of Power Sources. 2012;**204**:162-167

[15] Wu MS, Wang MJ, Jow JJ, Yang WD, Hsieh CY, Tsai HM. Electrochemical fabrication of anatase TiO(2) nanostructure as an anode material for aqueous lithium-ion batteries. Journal of Power Sources. 2008;**185**(2):1420-1424

[16] Kim J, Cho J. Rate characteristics of anatase TiO₂ nanotubes and nanorods for lithium battery anode materials at room temperature. Journal of the Electrochemical Society. 2017;**154**(6):A542-A546

[17] Zhang MH, Yin KB, Hood ZD, Bi ZH, Bridges CA, Dai S, et al. In situ TEM observation of the electrochemical lithiation of N-doped anatase TiO₂ nanotubes as anodes for lithium-ion batteries. Journal of Materials Chemistry A. 2017;**5**(39):20651-20,657

[18] Luo Y, Li J, Huang JG. Bioinspired hierarchical nanofibrous silver-nanoparticle/anatase-rutile-titania composite as an anode material for lithium-ion batteries. Langmuir. 2016;**32**(47):12338-12,343

[19] Yang XJ, Teng DH, Liu BX, Yu YH, Yang XP. Nanosized anatase titanium dioxide loaded porous carbon nanofiber webs as anode materials for lithium-ion batteries. Electrochemistry Communications. 2011;**139**(10):1098-1101

[20] Wu FX, Li XH, Wang ZX, Guo HJ, Wu L, Xiong XH, et al. A novel method to synthesize anatase TiO₂ nanowires as an anode material for lithium-ion batteries. Journal of Alloys and Compounds. 2011;**509**(18):3711-3715

[21] Lai C, Li CGRY, Dou Y, Gao XP. Mesoporous polyaniline or polypyrrole/anatase TiO₂ nanocomposite as anode materials for lithium-ion batteries. Electrochimica Acta. 2010;**55**(15):4567-4572

[22] Cheng XL, Hu M, Huang R, Jiang JS. HF-free synthesis of anatase TiO₂ nanosheets with largely exposed and clean {001} facets and their enhanced rate performance as anodes of lithium-ion battery. ACS Applied Materials and Interfaces. 2014;**6**(2):19176-19,183

[23] Roy P, Srivastava SK. Nanostructured anode materials for lithium ion batteries. Journal of Materials Chemistry A. 2015;**3**(6):2454-2484

[24] Wang XD, Li ZD, Shi J, Yu YH. One-dimensional titanium dioxide nanomaterials: Nanowires, nanorods, and nanobelts. Chemical Reviews. 2014;**114**(19):9346-9384

[25] Ortiz GF, Hanzu I, Djenizian T, Lavela P, Tirado JL, Knauth P. Alternative Li-ion battery electrode based on self-organized titania nanotubes. Chemistry of Materials. 2009;**21**(1):63-67

[26] Sudant G, Baudrin E, Larcher D, Tarascon JM. Electrochemical lithium reactivity with nanotextured anatase-type TiO₂. Journal of Materials Chemistry. 2005;**15**(12):1263-1269

[27] Wagemaker M, Borghols WJH, van Eck ERH, Kentgens APM, Kearley GL, Mulder FM. The influence of size on phase morphology and Li-ion mobility in nanosized lithiated anatase TiO₂. Chemistry--A European Journal. 2007;**13**(7):2023-2028

[28] Wagemaker M, Van Well AA, Kearley GJ, Mulder FM. The life and times of lithium in anatase TiO₂. Solid State Ionics. 2004;**175**(1):191-193

[29] He YB, Liu M, Xu ZL, Zhang B, Li B, Kang F, et al. Li-ion reaction to improve the rate performance of nanoporous anatase TiO₂ anodes. Energy Technology. 2013;**1**(11):668-674

[30] Macklin WJ, Neat RJ. Performance of titanium dioxide-based cathodes in

a lithium polymer electrolyte cell. Solid State Ionics. 1992;**53**:694-700

[31] Zhu GN, Wang YG, Xia YY. Ti-based compounds as anode materials for Li-ion batteries. Energy and Environmental Science. 2012;**5**(5):6652-6667

[32] Zhou ZY, Tian N, Li JT, Broadwell I, Sun SG. Nanomaterials of high surface energy with exceptional properties in catalysis and energy storage. Chemical Society Reviews. 2011;**40**(7):4167-4185

[33] Bavykin DV, Friedrich JM, Walsh FC. Protonated titanates and TiO_2 nanostructured materials: Synthesis, properties, and applications. Advanced Materials. 2006;**18**(2):2807-2824

[34] Zakharova GS, Jahne C, Popa A, Taschner C, Gemming T, Leonhardt A, et al. Anatase nanotubes as an electrode material for lithium-ion batteries. Physical Chemistry C. 2012;**116**(15):8714-8720

[35] Wagemaker M, Kentgens APM, Mulder FM. Equilibrium lithium transport between nanocrystalline phases in intercalated TiO_2 anatase. Nature. 2002;**418**(6896):397-399

[36] Hu YS, Kienle L, Guo YG, Maier J. High lithium electroactivity of nanometer-sized rutile TiO_2. Advanced Materials. 2006;**18**(11):1421-1426

[37] Murphy DW, Greenblatt M, Zahurak SM, Cava RJ, Waszczak JV, Hull GW, et al. Lithium insertion in anatase - a new route to the spinel $LiTi_2O_4$. Chemischer Informationsdienst. 1982;**19**(4-5):441-449

[38] Wagemaker M, Kearley GJ, van Well AA, Mulka H, Mulder FM. Multiple li positions inside oxygen octahedra in lithiated TiO_2 anatase. Journal of the American Chemical Society. 2003;**125**(3):840-848

[39] Jiang C, Zhang J. Nanoengineering titania for high rate lithium storage: A review. Journal of Materials Science and Technology. 2013;**29**(2):97-122

[40] Fröschl T, Hörmann U, Kubiak P, Kucerova G, Pfanzelt M, Weiss CK, et al. Nanoengineering titania for high rate lithium storage: A review. Journal of Royal Society of Chemistry. 2012;**41**(15):5313-5360

[41] Kavan L, Kalbac M, Zukalova M, Exnar I, Lorenzen V, Nesper R, et al. Lithium storage in nanostructured TiO_2 made by hydrothermal growth. Chemistry of Materials. 2004;**16**(3):477-485

[42] Lafont U, Carta D, Mountjoy G, Chadwick AV, Kelder EM. In situ structural changes upon electrochemical lithium insertion in nanosized anatalse TiO_2. Physical Chemistry C. 2010;**114**(2):1372-1378